Single-atom nanozymes

May 14 2019, by Thamarasee Jeewandara

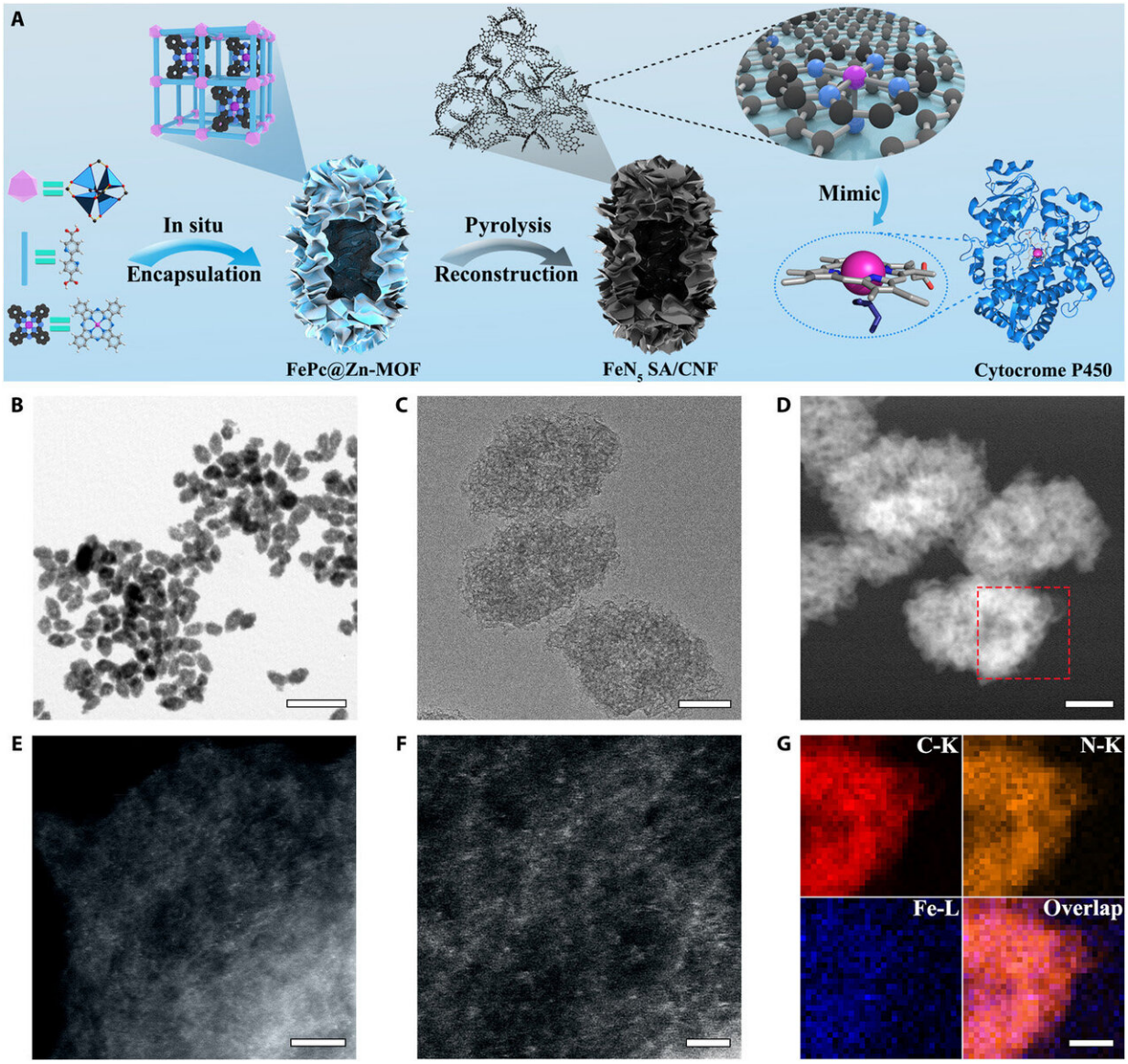

Synthetic scheme and morphology characterization of FeN5SA/CNF. (A) Schematic formation process of carbon nanoframe–confined atomically dispersed Fe sites with axial five-N coordination to mimic the active center of

cytocrome P450. (B and C) TEM images and (D) high-angle annular dark-field STEM (HAADF-STEM) image of FeN5 SA/CNF. (E and F) Magnified HAADF-STEM images of FeN5 SA/CNF showing the dominant metal single atom. (G) EELS mapping images of FeN5 SA/CNF of the selected region in (D). Scale bars, 1 μm and 100, 100, 5, 2, and 50 nm (B to G, respectively). Credit: Science Advances, doi: 10.1126/sciadv.aav5490.

Nanozymes are catalytic nanomaterials with enzyme-like characteristics that have attracted enormous recent research interest. The catalytic nanomaterials offer unique advantages of low cost, high stability, tunable catalytic activity and ease of mass production and storage. These properties are highly desirable for a wide range of applications in biosensing, tissue engineering therapeutics and environmental protection. However, conventional nanozyme technologies face critical challenges relative to their size, composition and facet-dependent catalysis, in addition to inherently low active site density.

Now writing in *Science Advances*, Liang Huang and co-workers at the departments of Electroanalytical Chemistry and Physics in China detail the discovery of a new class of single-atom enzymes with atomically dispersed enzyme-like active sites in nanomaterials. The sites significantly enhanced the catalytic performance of the single atom nanozymes and the scientists uncovered their underlying mechanism using oxidase catalysis as a model experimental reaction alongside theoretical calculations. They revealed the catalytic activities and behavior of single-atom nanozymes containing a carbon nanoframe (single atom/carbon nanoframe: SA/CNF) and confined FeN_5 active centers (FeN_5 SA/CNF) to mimic the natural axial ligand-coordinated heme of cytochrome P450 for versatile antibacterial applications. The results suggest that the single-atom nanozymes have great potential to become the next-generation nanozymes for applications in

nanobiotechnology.

Since discovering the peroxidase-like activity of ferromagnetic nanoparticles in 2007, scientists have engineered various nanozymes using materials such as metal oxides, noble metals, carbon materials and metal-organic frameworks (MOFs). However, two contemporary challenges remain in nanozyme technologies, where (1) the low density active sites showed lower catalytic activity compared with natural enzymes, and (2) the inhomogeneous elemental composition could complicate catalytic mechanisms. Due to these bottlenecks, scientists have found it challenging to discover the precise sites and origin of enzymatic activity, restricting extensive applications of conventional nanozymes.

In the present work, Huang and co-workers aimed to resolve these issues by discovering a new class of single-atom nanozymes incorporating state-of-the-art single-atom technology to engineer inherent enzyme-like active sites. The scientists showed that the atomically dispersed metal centers maximized the efficiency and density of active sites in the new nanozymes architecture. They used the well-defined coordination structure to provide a clear experimental model during investigations of its working mechanism. Huang et al. reported an effective and general method to synthesize the highly active single-atom nanozymes by mimicking the spatial structures of active centers in natural enzymes.

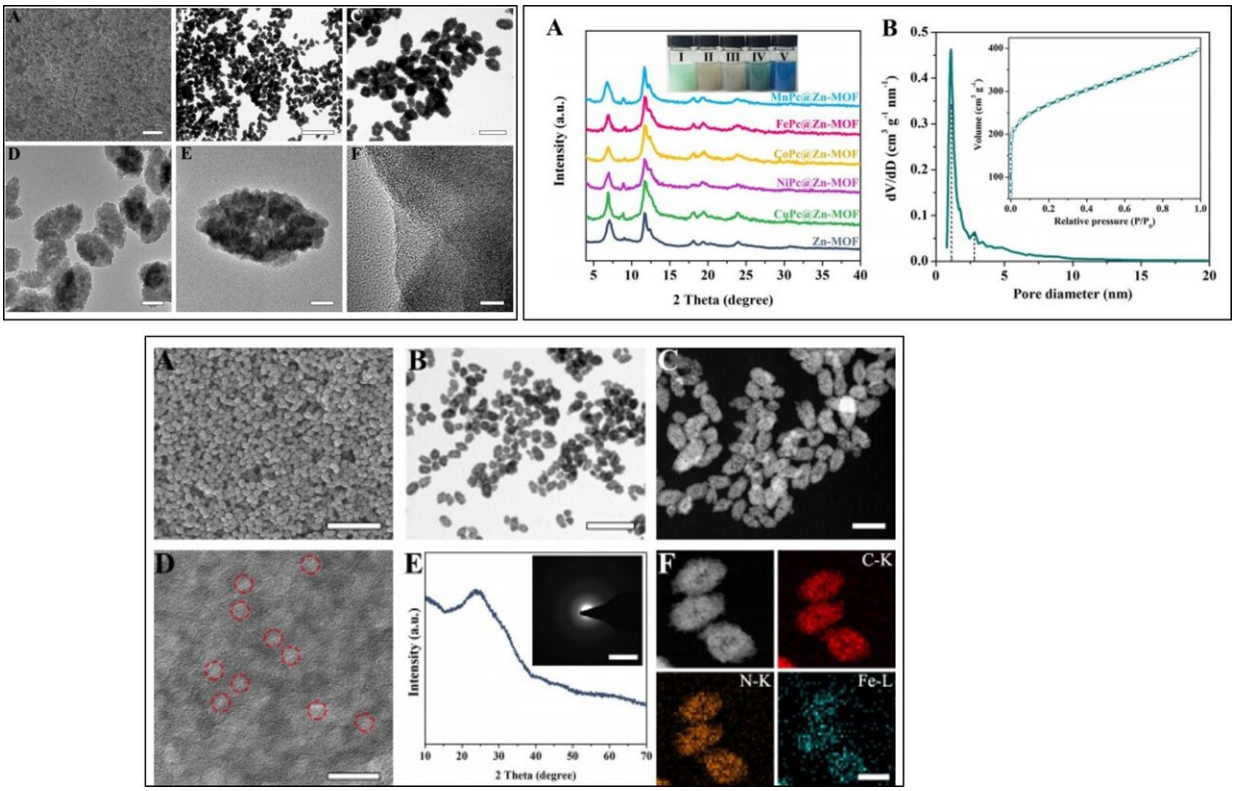

TOP LEFT: Morphology of the Zn-MOF precursor. (A) SEM image and (B) TEM image of ZnMOF. (C, D) TEM images and (E, F) HRTEM images of FePc@Zn-MOF. TOP RIGHT: Structure of the Zn-MOF precursor. (A) XRD pattern of MnPc@Zn-MOF (I), FePc@Zn-MOF (II), CoPc@Zn-MOF (III), NiPc@Zn-MOF (IV), CuPc@Zn-MOF (V) and ZnMOF. Inset is the optical image of the corresponding MPc@Zn-MOF in ethanol solution (10 mg mL-1). (Photo Credit: Liang Huang, Changchun Institute of Applied Chemistry) (B) Pore size distribution of FePc@Zn-MOF, and the inset of (B) is the corresponding N2 adsorption/desorption isotherms. BOTTOM: Morphology and structure of FeN5 SA/CNF. (A) SEM image, (B) TEM image, (C) STEM image, (D) HRTEM image, (E) XRD pattern and (F) TEM-EDS elemental mapping images of FeN5 SA/CNF. The porous structure in (D) is indicated by circles. The inset of (E) is corresponding SAED pattern. Credit: Science Advances, doi: 10.1126/sciadv.aav5490.

They used oxidase catalysis as a model reaction and completed theoretical calculations as well as experimental studies. The scientists identified the highest oxidase-like activity of FeN_5 SA/CNF to result via the synergistic effect and electron donor mechanism. Of note, FeN_5 SA/CNF showed more than 17-to-70 times higher oxidase-like activity compared to square planar FeN_4 catalyst and the commercial Pt/C (platinum on carbon catalyst) with normalized metal content. The results explained the unexpected oxidase-like push effect of axial coordination in FeN_5 SA/CNF and its significantly enhanced catalytic activity, compared to the conventional nanozymes.

To synthesize the FeN_5 SA/CNF, Huang et al. first designed a host-guest structure of metal-organic framework (MOF)-encapsulated iron phthalocyanine (FePc: FePc@Zn-MOF). This structure could host diverse metals to replace iron phthalocyanine (FePc) in later experiments as MPc where M ranged from manganese (MnPc), nickel (NiPc), copper (CuPc) to cobalt (CoPc) and pyrolyzed the precursor at 900^0C under nitrogen gas to obtain the single atom nanozymes.

The scientists had previously demonstrated that square planar FeN_4 sites would be retained during iron porphyrin and FePc (iron phthalocyanine) calcination reactions but in the absence of support, the monodispersed sites agglomerated into nanoparticles. In the present synthetic process therefore, the scientists isolated the FeN_4 sites confined in the carbon nanoframes and coordinated them with the pyridinic nitrogen (N) substrate to generate the more thermodynamic and stable FeN_5/C sites.

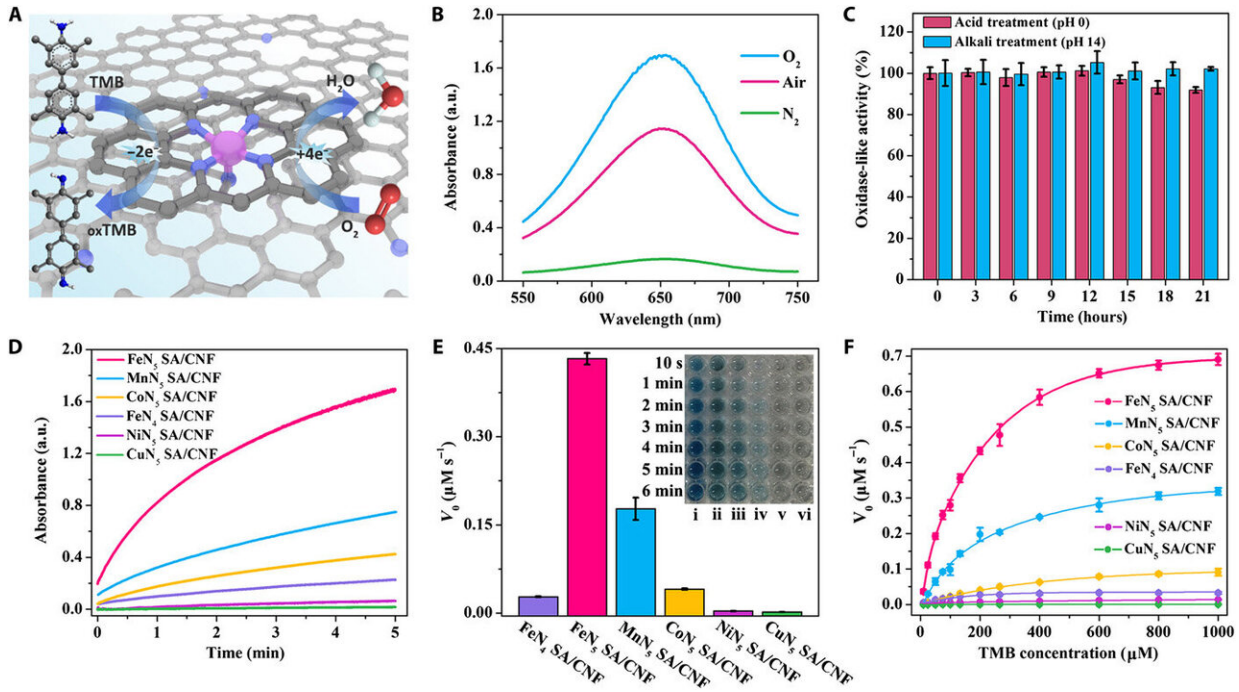

Oxidase-like activity of FeN5SA/CNF. (A) Schematic illustration of oxidase-like characteristics of FeN5 SA/CNF–catalyzed TMB oxidation. (B) Ultraviolet-visible (UV-vis) absorption spectra of FeN5 SA/CNF in O2-saturated, air-saturated, and N2-saturated sodium acetate–acetic acid buffer. (C) The durability of FeN5 SA/CNF treated with acid (alkali) for 21 hours. (D) Time-dependent absorbance changes at 652 nm, (E) histogram of V0, and (F) typical Michaelis-Menten curves in the presence of FeN5 SA/CNF (i), MnN5 SA/CNF (ii), CoN5 SA/CNF (iii), FeN4 SA/CNF (iv), NiN5 SA/CNF (v), and CuN5 SA/CNF (vi) in air-saturated sodium acetate–acetic acid buffer. The inset of (E) is an optical image of the TMB solution catalyzed by corresponding catalysts. Photo credit: Liang Huang, Changchun Institute of Applied Chemistry. Credit: Science Advances, doi: 10.1126/sciadv.aav5490

The scientists then characterized the morphology and structure of FeN_5 SA/CNF using scanning electron microscopy (SEM) and transmission electron microscopy (TEM) to reveal the fusiform FePc@Zn-MOF as a dominant product with uniform morphology. They observed that the

hollow cavities and porous shells endowed the substrate with high specific surface areas and abundant hierarchical nanopores.

The X-ray diffraction patterns (XRD) indicated that the crystal structure of Zn-MOF did not undergo significant changes after encapsulating FePc in situ, while the Fourier transform infrared (FTIR) spectrum of FePc@Zn-MOF verified successful encapsulation of FePc. Then by using electron energy-loss spectroscopy mapping, the scientists showed that the Fe and N atoms were homogenously distributed throughout the whole-domain, indicating the generation of Fe-N sites in 3-D matrices.

Huang et al. analyzed the atomic structure of FeN_5 SA/CNF to show that the coordination number of the Fe atom was nearly five – to confirm the formation of five Fe-N_5 moieties. To understand the structure underlying the catalytic mechanisms, the scientists also used Mössbauer spectroscopy (used to determine the oxidation state of iron) and investigated the electron structure and iron (Fe) coordination. They then determined the oxidase-like activities of FeN_5 SA/CNF using colorimetric assays and used the oxidation of TMB (3,3,5,5-tetramethylbenzidine) as a model catalytic reaction to understand the interaction of oxygen molecules with FeN_5 SA/CNF in various environments.

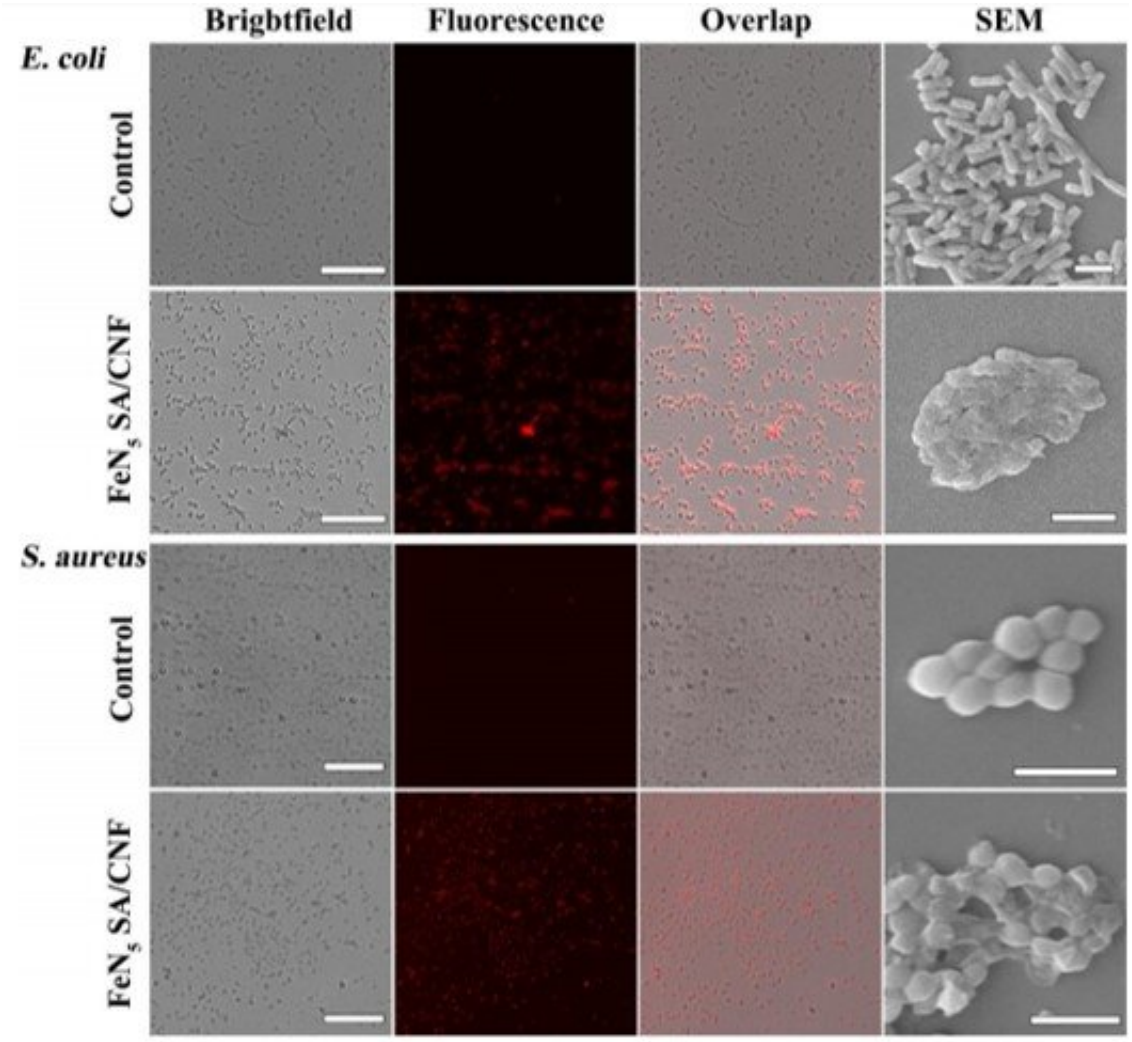

Morphological changes in bacteria. Brightfield images, Fluorescence images, overlap images and SEM images of E. coli and S. aureus bacteria treated or untreated with FeN5 SA/CNF. The scale bars are 40 μm for fluorescence images and 2 μm for SEM images. Credit: Science Advances, doi: 10.1126/sciadv.aav5490

The results showed the intense catalytic activity of FeN_5 SA/CNF during reduction of oxygen and the scientists credited the oxidation rate of TMB to the concentration of oxygen. Huang et al. then comparatively studied the oxidase-like activities of FeN_5 SA/CNF vs. MN_5 SA/CNF

where they replaced M with different metals of Mn, Fe, Co, Ni and Cu. They showed the catalytic rate of FeN_5 SA/CNF to be the highest (17 orders higher than FeN_4 SA/CNF) via distinct color changes across time.

When Huang et al. compared the enzymatic activity with conventional enzymes used previously, they observed that FeN_5 SA/CNF maintained comparatively far superior oxidase-like activity. Of note, the catalytic rate of the new nanozymes were 70 times greater than the commercial Pt/C. Based on the experimental results, the scientists validated that mechanistically the central metal atom and axial five-N-coordinated structure were important for the superior oxidase-like activities of single-atom nanozymes.

As a practical application of high-oxidation catalytic activity, the single-atom nanozymes of FeN_5 SA/CNF could generate reactive oxygen species during the catalytic reduction of oxygen, which can impair the membrane of bacteria for effective antibacterial actions. To assess antibacterial activity, Huang et al. conducted in vitro experiments and detected the survival rates of *Escherichia coli* and *Staphylococcus aureus* cells on exposure to the nanozymes. On comparison with a control group, the scientists observed markedly reduced bacterial survival rates; substantiating high oxidase-like activities of FeN_5 SA/CNF for significant antibacterial activity.

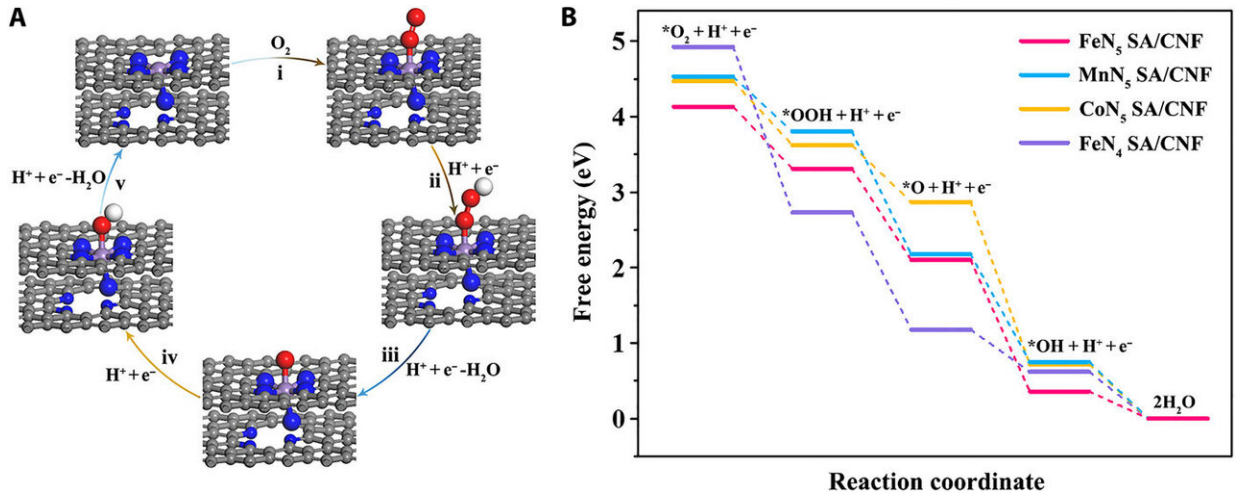

Theoretical investigation of oxidase-like activity over FeN5SA/CNF. (A) Proposed reaction pathways of O2 reduction to H2O with optimized adsorption configurations on FeN5 SA/CNF. The gray, blue, purple, red, and white balls represent the C, N, Fe, O, and H atoms, respectively. (B) Free energy diagram for oxygen reduction reaction on single-atom enzyme mimics with TMB as reductant in an acidic medium. Credit: Science Advances, doi: 10.1126/sciadv.aav5490

Based on the in vitro experimental outcomes, the scientists next conducted in vivo antibacterial studies using the new nanozymes. For this, they used a wound infection model of mice to understand the antibacterial efficacy of FeN_5 SA/CNF. After 4-days of infecting a wound site with E. coli followed by nanozyme therapy, Huang et al. observed the clear remission of ulceration and accelerated wound healing in the treatment group.

The scientists verified the in vivo healing process using histopathology studies of the wounded tissue stained with hematoxylin and eosin. The results showed that keratinocytes migrated to the wound site from the normal tissue, to thicken the epidermis after treatment, confirming a

highly biocompatible bacterial nanozyme. As before, Huang et al. credited the results to the architecture of atomically dispersed FeN_5 sites, as actual active centers in these catalysts.

To determine the precise origin of the enhanced oxidase-like activity of the FeN_5 SA/CNF using theoretical calculations, Huang et al. performed density functional theory (DFT) calculations. For this, they used the oxygen molecular reduction process of single-atom metal sites, with TMB molecules as the reducing agent in acidic conditions. The scientists showed that compared with the starting square planar FeN_4 SA/CNF, the axial-coordinated N atom used to form FeN_5 SA/CNF provided a strong push effect in the nanozymes architecture; to activate the oxygen molecule and cleave the O-O bond. This process promoted the oxidative capacity of the single atom nanozymes, to acquire acidic hydrogens from substrates such as TMB, while oxidizing them. Thereby, based on the DFT calculations, Huang et al. unmistakably credited the origin of the superior oxidase-like activity to the central metal atom and the steric configurations of single-atom nanozymes.

In this way. Huang and colleagues reported the discovery of a new class of single-atom nanozymes with atomically dispersed enzyme-like active sites in nanomaterials. The new nanozymes showed significantly superior catalytic performance compared with conventional nanozymes in the lab. The observations resulted in uncovering their underlying mechanism during the study, using oxidase catalysis as a model reaction. Using both experimental studies and theoretical calculations, the scientists revealed the electron-push effect mechanism crucial to endow FeN_5 SA/CNF with the characteristically superior oxidase-like activity, compared to other nanozymes. This led to efficient bactericidal investigations and wound disinfection in vitro and in vivo. The scientists present a new perspective to the catalytic mechanisms and rational design of nanozymes to exhibit great potential and predict the origin of a next-generation nanozyme.

More information: Lizeng Gao et al. Intrinsic peroxidase-like activity of ferromagnetic nanoparticles, *Nature Nanotechnology* (2007). DOI: 10.1038/nnano.2007.260

Bing Jiang et al. Standardized assays for determining the catalytic activity and kinetics of peroxidase-like nanozymes, *Nature Protocols* (2018). DOI: 10.1038/s41596-018-0001-1

Citation: Single-atom nanozymes (2019, May 14) retrieved 12 May 2024 from https://phys.org/news/2019-05-single-atom-nanozymes.html